

High Aggregation Number Silver Clusters by Matrix-Assisted Laser Desorption/Ionization: Role of Matrixes on the Gas-Phase Reduction of Silver Ions

Sándor Kéki, László Sz. Szilágyi, János Török, György Deák, and Miklós Zsuga*

Department of Applied Chemistry, University of Debrecen, H-4010 Debrecen, Hungary

Received: November 11, 2002; In Final Form: January 27, 2003

Singly positively and negatively charged silver-cluster ions were effectively produced under matrix-assisted laser desorption/ionization (MALDI) conditions up to the aggregation number of $n \approx 200$, using reductive polar organic matrixes and silver trifluoroacetate (AgTFA). It was found that the matrix greatly influences the resulting cluster ion abundances. The effect of the matrixes with various chemical structures on the cluster formation was systematically investigated. It was also observed that the ion intensities decreased sharply at particular cluster numbers called “magic” numbers, independently of the matrix used, and this is in good agreement with the jellium model theory. The highest observed magic numbers were achieved with HABA [2-(4-hydroxyphenylazo)benzoic acid] and are 139 and 137 for positively and negatively charged cluster ions, respectively. The fragmentations of both singly positively and negatively charged clusters ions were also studied. It was found that even-number clusters lose one silver atom, while clusters with an odd-number emit a single or two silver atoms. The fragmentation behavior of clusters as a function of the cluster size is reported. On the basis of the results a possible mechanism for the cluster ion formation is also presented.

Introduction

Metal and metal-related clusters are of great importance from both theoretical¹ and practical² points of view. Investigation of cluster formation in the gas-phase by mass spectrometry provides valuable information on the stability and electronic properties of clusters of different sizes. This information can be utilized when the clusters are immersed into a liquid or solid environment. In the past decades several methods were explored to induce gas-phase generation of metal clusters, and most of these techniques were based on the evaporation of metals by heating^{3,4} or by laser^{5–7} and ion bombardment.^{8–11} Recently, the generation of silver-cluster ions in matrix-assisted laser desorption/ionization (MALDI)^{12,13} was reported using silver salts and all-trans retinoic acid (RTA) as the matrix¹⁴ and another acidic matrix.¹⁵ In the analysis of nonpolar polymers, such as polystyrene,¹⁶ polybutadiene,¹⁷ and polyisobutylene,¹⁸ often silver salts are added to the mixtures of matrix and analyte to enhance the cationization of these polymers. Since the cationization in the plume is highly affected by the silver cluster formation, as a continuation of our investigations to achieve well-resolved MALDI MS spectra of the highly unpolar telechelic polyisobutylene¹⁸ and other nonpolar polymers, we decided to find out and understand the role of matrixes in the mechanism of cluster formation. Sometimes, however, depending on the MALDI experimental conditions, signals originated from the Ag_n^+ clusters may strongly interfere with those of the (polymer + Ag)⁺, adduct ions,¹⁵ rendering the evaluation of mass spectral data very difficult. In a reverse case, however, the formation of Ag_n^+ and Ag_n^- clusters may be utilized for the production of a large number of cluster ions, making MALDI an effective ion source of these cluster ions for the study of, for example, cluster ion–molecule reactions.

On the other hand, fragmentations of different clusters give valuable information on their stability and electronic properties. The extension of the MALDI-TOF (time-of-flight) MS with the

so-called “postsources decay” method (PSD)^{19,20} offers the capability for the study of fragmentation of various materials. The operation of the PSD-MALDI-TOF MS/MS is based on the mass determination of the fragment ions formed from the decomposition of the selected precursor ions of high internal energy in the first field-free region of the reflectron time-of-flight type instruments.²¹

In this paper, we report a very efficient production of Ag_n^+ and Ag_n^- cluster ions up to the size $n \approx 200$ together with the dependence of the cluster ion intensity on the matrix using MALDI as the ion source. The highest “magic” numbers determined in this work are 139 and 137 for Ag_n^+ and Ag_n^- clusters, respectively. In addition, the fragmentation of cluster ion as a function of the cluster size is also reported.

Experimental Section

Materials. Matrixes 3,5-dimethoxy-4-hydroxycinnamic acid (Sinapinic acid, SA), *trans*-3-indoleacrylic acid (IAA), 1,8,9-trihydroxyanthracene (dithranol, DIT), 3-hydroxypicolinic acid (HPA), 2-(4-hydroxyphenylazo)benzoic acid (HABA), α -cyano-4-hydroxycinnamic acid (CHCA), 2-amino-5-nitropyridine (ANP), 1-methyl-7-methoxy-3,4-dihydro- β -carboline (Harmaline, HAR), 2,4,6-trihydroxyacetophenone (THAP), and 2,5-dihydroxybenzoic acid (DHB) were purchased from Aldrich (Germany) and used as received. Silver trifluoroacetate (AgTFA) were received from Aldrich (Germany) and used without further purification. Tetrahydrofuran (THF) from Aldrich was purified as described.²² Polystyrene (PS) standard ($M_n = 2200$ g/mol) was purchased from Merck (Germany).

Instruments. MALDI-TOF MS. The MALDI MS measurements were performed with a Bruker BIFLEX III mass spectrometer equipped with a TOF analyzer. In all cases a 19 kV total acceleration voltage was used with pulsed ion extraction (PIE). To achieve good resolution of cluster peaks in the mass range 700–2500 Da, a 3 kV pulse (extraction) voltage with a

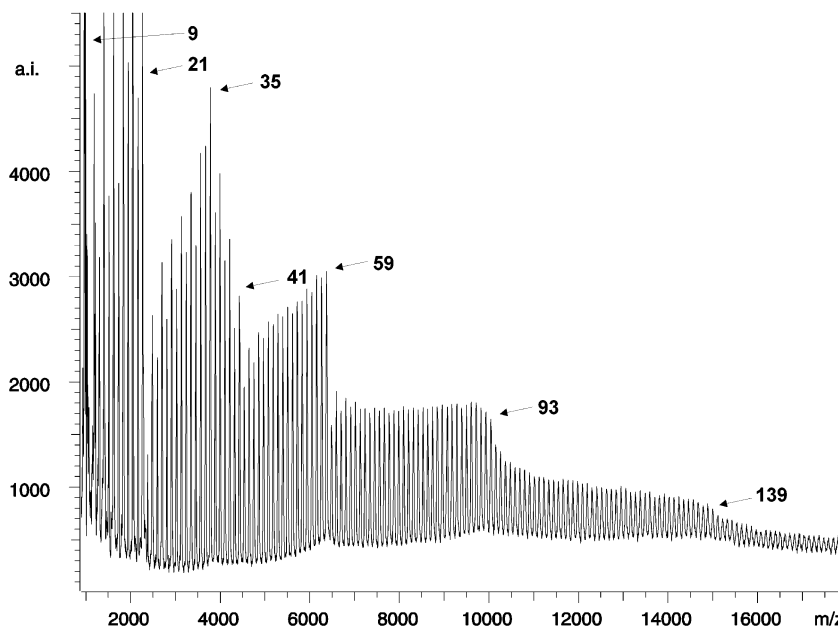


Figure 1. MALDI-TOF MS spectrum of a mixture of HABA and AgTFA recorded in the positive reflectron mode. Experimental conditions: 5:1 (v/v) mixture of HABA (0.08 M) and AgTFA (0.09 M) solutions.

delay time of 300 ns was applied. The ions were detected in both the linear and the reflectron mode. A LSI type nitrogen laser (337 nm, 10^6 to 10^7 W/cm², 3 ns pulse width) operating at 2 Hz was used to produce laser desorption, and 300–500 shots were summed. Matrixes were dissolved in THF in the concentration range 0.08–0.15 M. AgTFA dissolved in THF was used at the concentration 0.09 M. The ions were detected with a multichannel plate (MCP) detector at the voltage 1.65 kV. The spectra were externally calibrated with poly(ethylene glycol) (PEG) ($M_n = 1450$ g/mol, $M_w/M_n = 1.02$). The solutions of the matrix and AgTFA were mixed in a 5:1 v/v ratio (matrix/AgTFA). A volume of 0.5 μ L of these solutions was deposited onto the sample plate (stainless steel) and allowed to air dry.

PSD MALDI-TOF MS/MS. All of the PSD spectra were recorded by selection of the precursor ion to be studied, using the pulser allowing an approximately 20–30 Da window for selection. In these experiments a 19 kV total acceleration voltage and a 4.55 kV pulse voltage with a delay time of 100 ns were employed. In each segment of the spectrum accumulation, the reflectron voltage was decreased. The segments were pasted and calibrated using XMASS 5.0 software from Bruker. It is important to emphasize that the precursor ion in the range of cluster size $n = 9$ –25 and the fragment ions were recorded in the same segments, that is, in the first segment. The PSD was calibrated using the fragmentation pattern of adrenocorticotrophic hormone (ACTH) over the mass range 60–2450 Da.

FT-IR. FT-IR measurements were performed with a Perkin-Elmer Paragon 1000 PC instrument.

Results and Discussion

As was reported recently,¹⁵ acidity of the matrix is an important factor for obtaining silver clusters under MALDI conditions. HABA was found to be the most promising matrix to yield relatively high cluster ions up to m/z 7000 Da ($n \approx 65$). Surprisingly, upon using the HABA/AgTFA systems, we obtained highly resolved mass spectra of Ag cluster ions with much higher aggregation number in both the positive and negative reflectron modes (Figures 1 and 2).

The MALDI-TOF MS spectra presented in Figures 1 and 2 were obtained in a way that ions below m/z 700 (matrix, adduct

ions, small silver-cluster ions) were deflected in order to avoid saturation of the detector because of the high intensity of these ions. As shown in Figures 1 and 2, both in the positive and in the negative mode a series of peaks with a repeat mass of 108 Da appeared, which is characteristic of the average mass of silver. These observations indicate the presence of Ag_n^+ and Ag_n^- cluster ions. In the mass range m/z 700–2500 Da, isotopic resolution of peaks was obtained. To support the presence of pure silver cluster ions, the isotopic distributions of these peaks were compared with those calculated for the corresponding Ag_n^+ and Ag_n^- clusters. Figure 3 shows the observed and the calculated isotopic distributions for the Ag_9^+ cluster ions.

Figure 3 shows that there is good agreement between the observed and the calculated isotopic distributions, which supports the presence of pure silver-cluster ions. Similarly to the observation of Rashidzadeh et al.¹⁴ in the presence of an RTA matrix, one can recognize two characteristics of these mass spectra: (i) The ion intensity at odd–even cluster number oscillates; that is, the ion intensity of odd-number clusters is larger than that of the adjacent even-number cluster. (ii) A sharp decrease in the ion intensity at special cluster numbers was recognized. It is to be noted that in the presence of an RTA matrix the highest magic number was 59 in the positively charged clusters and 57 in the negatively charged clusters.¹⁴ On the other hand, in our case $n = 9, 21, 35, 41, 59, 93$, and 139 and $n = 19, 33, 39, 57, 91$, and 137 magic numbers were found for Ag_n^+ and Ag_n^- cluster ions, respectively. Furthermore, we observed local maxima in the ion intensities at $n = 35$ and 59 for the positively charged silver-cluster ions and $n = 33$ and 57 for the negatively charged silver-cluster ions. The observed peculiarities can be easily explained on the basis of the jellium model theory^{8,9,23} (JM). According to this theory, the stability of the cluster is mainly determined by the energy levels of valence electron bound in the cluster. Clusters containing an even-number of valence electrons possess higher stability due to spin–spin coupling than those having an odd-number of electrons bound in their electronic shell. On the other hand, clusters in which the shell is closed have higher stability than the neighboring clusters. The shell-closing effect occurs at the number of free electrons $n_s = 2, 8, 20, 34, 58, 92, 138$,

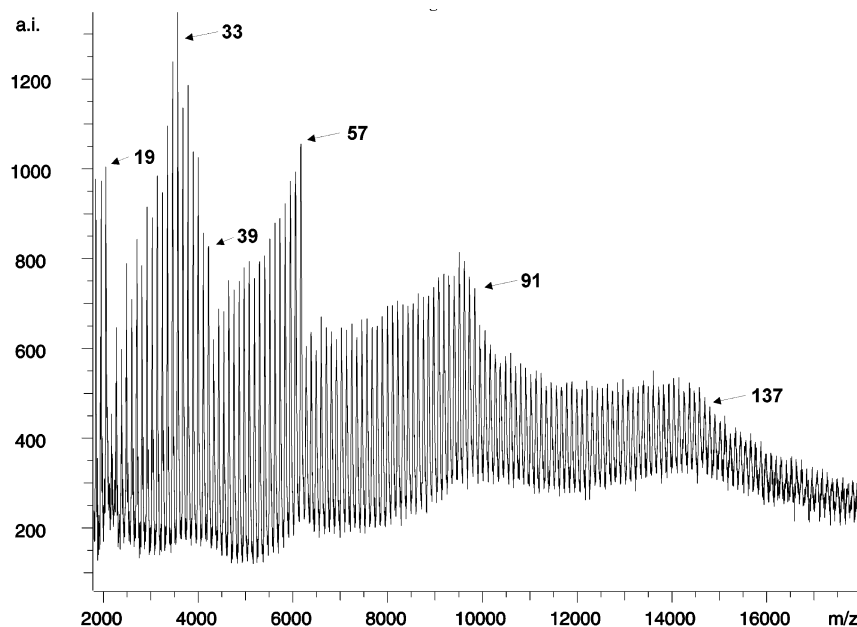


Figure 2. MALDI-TOF MS spectrum of a mixture of HABA and AgTFA recorded in the negative reflectron mode. Experimental conditions: 5:1 (v/v) mixture of HABA (0.08 M) and AgTFA (0.09 M) solutions.

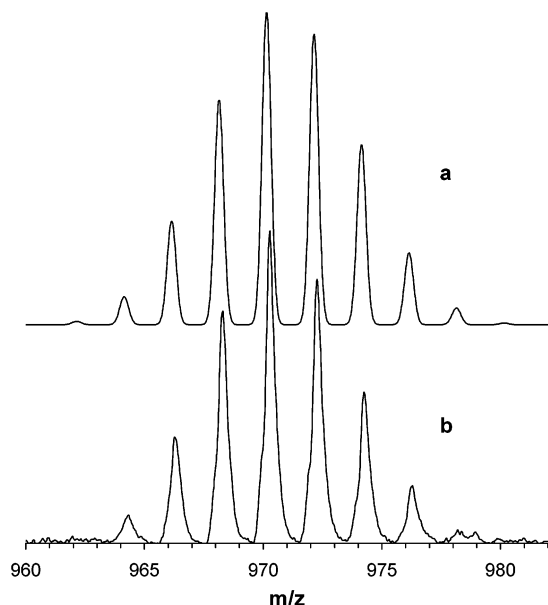


Figure 3. Calculated (a) and observed (b) isotopic distributions for Ag_n^+ cluster ions produced when using a mixture of HABA and AgTFA. The isotopic distributions were calculated by taking into account the Gaussian peak broadening with the experimental resolution (R) ($R = 2400$ fwhm (full width at half-maximum)). Experimental conditions: 5:1 (v/v) mixture of HABA (0.08 M) and AgTFA (0.09 M) solutions.

and 198. Therefore, the magic number (n_m), that is, the cluster number after which the ion intensity drops, can be expressed as

$$n_m = n_s + z \quad (1)$$

where z is the charge of the cluster.

The observed “magic” numbers for the Ag_n^+ and Ag_n^- cluster ions agree well with those predicted by the theory. The highest resolved cluster peaks were achieved up to the size $n \approx 200$ for both the positive and negative ions; however, we were not able to experimentally determine the next magic numbers at $n_m = 199$ (for positive ions) and $n_m = 197$ (for negative ions)

because of the poor signal-to-noise ratio in this region. On the other hand, the sharpness of the intensity drops as magic numbers decrease with the increasing cluster number, especially above 57 and 59. Odd–even alternation and magic numbers were also found in the case of metal clusters obtained by ion bombardment^{8–10} and other methods.²³ It has been found in the ion-bombardment experiments that the intensity of the cluster ions ($I(n)$) obeys the power law^{9,11} $I(n) = n^{-\delta}$. Considering our systems, although the ion intensity decreases with increasing cluster size, it seems to be far from scaling with such a power law, which may indicate a different cluster formation mechanism. On the other hand, we found that the laser fluence also affects the ion abundances. At low laser fluence, but above the threshold, no significant formation of silver clusters can be observed. Cluster ions begin to appear at higher laser fluence.

Fragmentation of Silver-Cluster Ions. Besides the major peaks in the positive reflectron MALDI-TOF MS spectrum obtained with the HABA/AgTFA sample (Figure 1), a series of minor peaks with low intensity occurred differing by ~ 11 Da in mass from the main series. Although all of the peaks in the mass range 700–2500 Da are isotopically resolved, the resolutions of these minor peaks are considerably lower than those of the adjacent major peaks. These observations indicate that the minor, low intensity peaks may be due to the fragmentation of silver cluster ions in the flight tube of the instruments. To support this, the MALDI-TOF MS spectra were recorded in the linear mode, too. The overlaid zoomed spectra recorded in the reflectron and in the linear mode are shown in Figure 4.

Figure 4 shows that the minor peaks in the linear spectrum disappeared, which strongly confirms that these peaks in the reflectron spectrum are originated from the fragment ions formed from the silver-cluster ions in the flight tube, that is, by postsource decay (PSD).^{19,20} It should be kept in mind that the fragment ions and their precursor ions cannot be differentiated in the linear mode, since both of them have the same flight time. To study the fragmentation of silver cluster ions, cluster ions with size to be investigated as precursor ions were selected for PSD. The selection was made at the cluster size $n = 9–25$. Since it was observed that the fragmentation patterns of even-

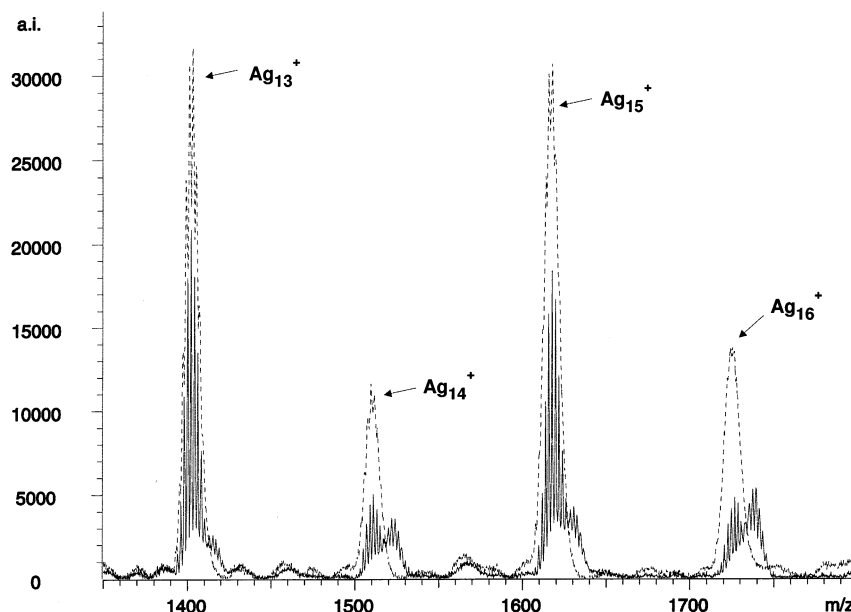


Figure 4. MALDI-TOF MS spectrum of a mixture of HABA and AgTFA recorded in the positive reflectron (—) and the linear (---) modes. Experimental conditions: 5:1 (v/v) mixture of HABA (0.08 M) and AgTFA (0.09 M) solutions.

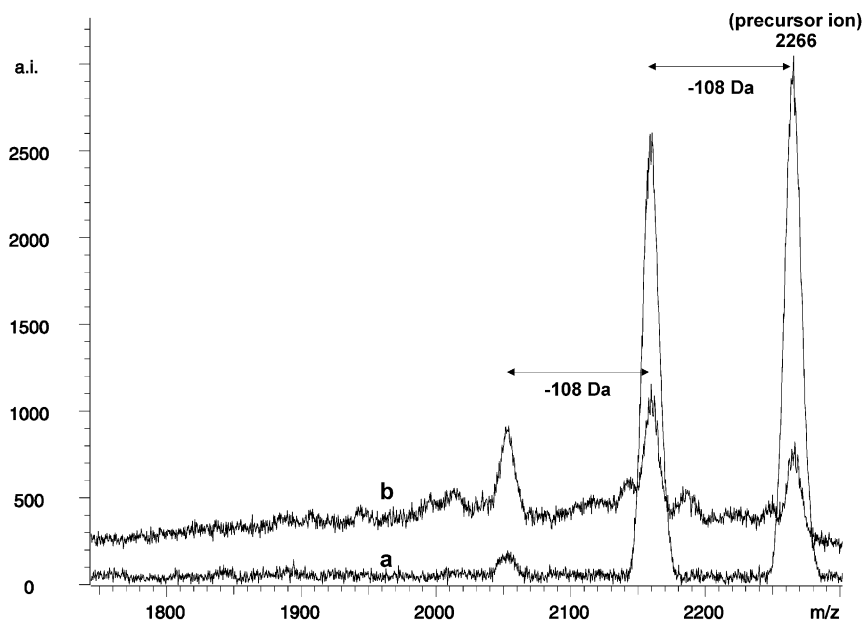


Figure 5. PSD-MALDI-TOF MS/MS spectra of Ag_{21}^+ (a) and Ag_{21}^- (b) cluster ions generated from the mixture of HABA and AgTFA. Experimental conditions: 5:1 (v/v) mixture of HABA (0.08 M) and AgTFA (0.09 M) solutions.

and odd-sized negatively and positively charged clusters are different, we discuss the results according to this finding. The PSD spectra of even-sized clusters showed the formation of Ag_{2m-1}^+ fragment ions produced by loss of a single silver atom from Ag_{2m}^+ ($n = 2m$). This is the only fragment ion that can be found in these spectra, and no other peaks of fragment ions appeared in the lower mass region of the PSD spectra. The same holds for the even-number, negatively charged cluster ions, that is, even-sized cluster ions; independently of their charge state, they emit a single atom to form the next smaller cluster. Similar results were obtained by laser vaporization^{24–26} and ion-bombardment^{9,27} experiments. It was also found in our PSD experiments that the intensity of the fragment ions with respect to those of the precursor ions increased with the increasing cluster size. As mentioned before, the fragmentation process of odd-number clusters is different from those of the even-sized clusters.

Figure 5 shows the PSD-MALDI-TOF MS/MS spectra of Ag_{21}^+ and Ag_{21}^- . As is evident from Figure 5, the presence of two fragment ions formed by loss of a single (Ag_{20}^+ and Ag_{20}^-) or two silver atoms (Ag_{19}^+ and Ag_{19}^-) can be recognized for both Ag_{21}^+ and Ag_{21}^- . It is also seen in Figure 5 that the intensities of the fragment ions formed by the emission of two Ag atoms with respect to those of their precursor ions are much higher in the case of Ag_{21}^- than for Ag_{21}^+ . The intensity differences in the PSD spectra of Ag_{21}^- and Ag_{21}^+ are due to the fact that in the case of Ag_{21}^- a stable Ag_{19}^- fragment ion is formed, while in the case of Ag_{21}^+ a stable cluster ion is fragmented into a less stable cluster ion. Therefore, the PSD spectrum of Ag_{21}^- considering the corresponding fragment ion intensities (Figure 5b) is rather similar to those of Ag_{23}^+ (Figure 6).

Figure 7 shows the intensities of the fragment ions produced by the loss of a single (r_{-1}) and two Ag atoms (r_{-2}) compared

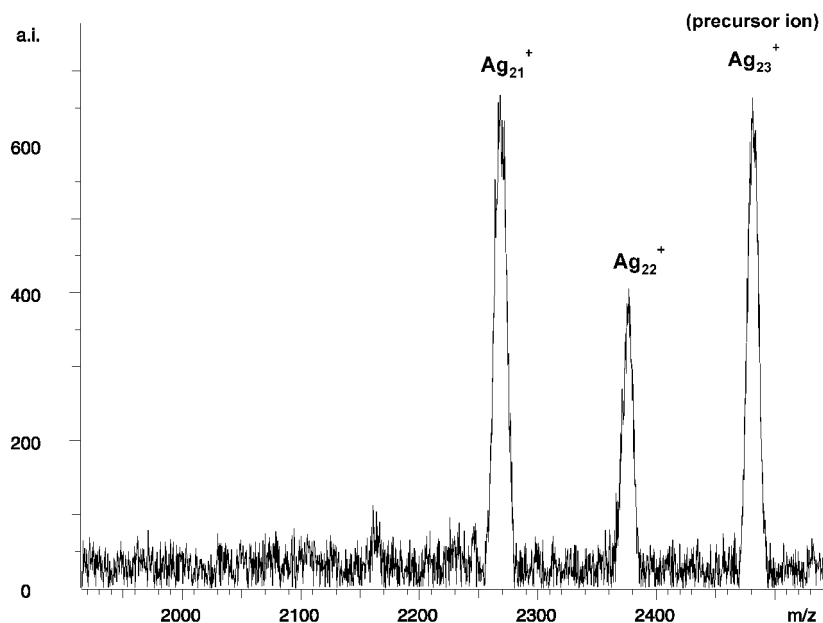


Figure 6. PSD-MALDI-TOF MS/MS spectra of Ag_{23}^+ cluster ion generated from the mixture of HABA and AgTFA. Experimental conditions: 5:1 (v/v) mixture of HABA (0.08 M) and AgTFA (0.09 M) solutions.

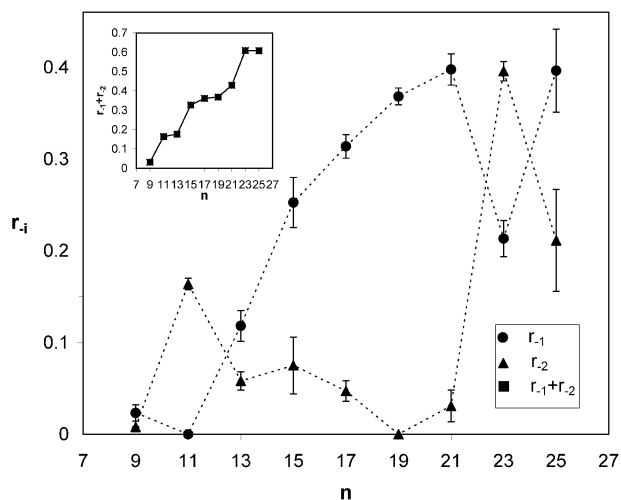


Figure 7. Dependences of the fragment ion yields on the positively charged clusters of the odd-number. $r_{-1} = I_{-1}/(I_{-1} + I_{-2} + I_p)$ and $r_{-2} = I_{-2}/(I_{-1} + I_{-2} + I_p)$, where I_{-1} and I_{-2} are the intensity of fragment ion formed by loss of a single and two Ag atoms, respectively. I_p stands for the intensity of the precursor ion.

to the total ion intensities (including those of the precursor ions) as a function of the odd-number cluster size.

As seen in Figure 7 there are some peculiarities on these curves. The intensity of fragment ions formed by the loss of a single silver atom (r_{-1}) shows minima while that of the fragment ions produced by the emission of two Ag atoms (r_{-2}) reveals maxima at cluster numbers 11 and 23. The total fragment ion intensity ($r_{-1} + r_{-2}$) increases monotonically with the increasing cluster size with steps at sizes of $n = 11$ and 23. These results indicate that the fragmentations of Ag_{23}^+ to Ag_{21}^+ and Ag_{11}^+ to Ag_9^+ are preferred, owing to the formation of clusters with magic numbers (because of the high stability of these “magic” clusters). The single negatively charged cluster ions showed similar fragmentation patterns, but the increase in the intensity of the fragment ions formed by the loss of two Ag atoms (r_{-2}) occurred at a cluster size smaller by 2 than those for the positively charged cluster ion. This finding also revealed the preferential fragmentation of Ag_{21}^- to Ag_{19}^- (the magic number for negatively charged clusters is 19).

However, it is also seen in Figure 7 that no formation of fragment ion formed from Ag_{11}^+ by emission of a single Ag atom appeared; that is, only the presence of Ag_{10}^+ can be recognized. We have also performed PSD experiments at the cluster size $n = 3-7$. Although the background in the region of these low mass cluster ions was very high due to the presence of a matrix, adduct ions, and other fragment ions, it was possible to select these cluster ions for PSD. According to these investigations, Ag_3^+ , Ag_5^+ , and Ag_7^+ fragment to the next smaller cluster ions having two Ag atoms less than (i.e., $\text{Ag}_3^+ \rightarrow \text{Ag}^+$, $\text{Ag}_5^+ \rightarrow \text{Ag}_3^+$ and $\text{Ag}_7^+ \rightarrow \text{Ag}_5^+$) their precursors (similarly to those of Ag_{11}^+ , that is, $\text{Ag}_{11}^+ \rightarrow \text{Ag}_9^+$). No sign of loss of a single silver atom can be recognized at these cluster sizes ($n = 3, 5, 7$, and 11). These observations indicate that the emission of dimer (Ag_2) dominates over the successive loss of two silver atoms as the cluster size decreases. This result corroborates well with that obtained by the laser vaporization method using collision induced dissociation (CID) excitation for fragmentation of silver clusters.^{24,25} It has been shown²⁴ that the evaporation of the dimer from clusters Ag_n^+ is energetically favored over the loss of single Ag atoms if relation 2 is fulfilled.

$$E_D(n-1)^+ < E_D(\text{Ag}_2)^0 \quad (2)$$

where $E_D(n-1)^+$ and $E_D(\text{Ag}_2)^0$ are the dissociation energy of the cluster Ag_{n-1}^+ (next smaller cluster) and that of the neutral dimer, respectively.

The values of the dissociation energies for the Ag_2 dimer²⁸ and for Ag_n^+ (refs 25 and 26) in the range $n = 2-25$ have been determined experimentally, and it was found that relation 2 is fulfilled in the case of cluster size $n = 3, 5, 7$, and 11, but not for $n = 9$. Our experiments performed under MALDI conditions support these findings. Interestingly, we have found fragment ions with very low intensity formed by the loss of four Ag units from the clusters of $n = 7, 13$, and 25. The emission of four Ag units from these clusters results in the formation of “magic” clusters with $n = 3, 9$, and 21. This process seems to possess a high dissociation threshold, but it occurs under our MALDI experimental conditions, albeit with very low abundances.

TABLE 1: Characteristics of MALDI-TOF MS Spectra of the Mixture of Different Matrixes and AgTFA Obtained in the Positive (+) and in the Negative (−) Reflectron Modes^a

matrix	highest obs “magic” no. (+/−)	highest obs odd–even alteration (+/−)	highest resolved cluster no. (+/−)	overall signal intensity of clusters ^b
IAA	93/91	63/25	165/140	S/M
HPA ^c	93/19	51/7	140/19	M/W
DHB	93/57	43/31	140/120	M/M
THAP	59/19	35/13	65/25	W/W
ANP	41/19	23/11	45/21	W/W
CHCA	93/91	63/19	140/130	M/W
SA	59/19	57/15	100/30	M/W
DIT	59/7	45/11	65/15	W/W
HAR ^c	139/91	53/55	165/150	S/M
HABA	139/137	71/61	210/200	S/S

^a Experimental conditions: 5:1 (v/v) mixture of matrix (0.08 M) and AgTFA (0.09 M) solutions. During recording the spectra, the laser fluence was kept constant. ^b S = strong; M = medium; W = weak signal intensity. ^c saturated solutions in THF were used.

Dependence of the Cluster Formation on the Matrix. The silver cluster formation was investigated using different matrixes and AgTFA mixtures under the same experimental conditions, and the results are summarized in Table 1.

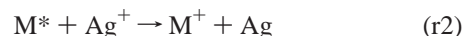
As it turns out from the data of Table 1, the matrix has a significant effect on the cluster formation. Ag_n^+ and Ag_n^- cluster ions can be effectively produced using HABA, HAR, IAA, and DHB. As expected, the overall signal intensities correlate with the highest observable magic numbers and the highest resolved cluster numbers. In the case of matrixes with which strong Ag_n^+ cluster ion formation was observed, the same was experienced for the formation of Ag_n^- cluster ions, except for HPA, where, despite the significant ion intensity of Ag_n^+ , only a very weak signal was obtained for Ag_n^- . It should be noted that the signal intensity of Ag_n^- was always lower than that of Ag_n^+ . In the case of equal detection efficiency for positive and negative ions, it can be concluded that the concentration of Ag_n^- in the plume is lower than that of Ag_n^+ . As a general trend in Table 1, it can be found that matrixes having carboxyl group(s) (e.g. HABA, DHB, IAA, CHCA) produce strong cluster ion signals, while matrixes with phenolic hydroxyl groups (DIT, THAP) or without the latter two groups (ANP) generate only a weak cluster ion signal. The exception in this trend is the HAR. The possible reason for this will be discussed later.

Possible Mechanism of Cluster Formation. In the absence of matrix, AgTFA, alone, does not produce a significant amount of cluster ions; only formation of small cluster ions up to the size $n = 9$ –13 can be observed. Upon addition of matrix to AgTFA, formation of larger cluster ion is enhanced. When the molar ratios of matrix to AgTFA were adjusted to 50:1 or 1:50, silver-cluster ion formations were also observed but with much lower abundances. Upon mixing the matrix and AgTFA solutions, immediately and after predetermined intervals (20 min interval, for 2 h), samples were taken from the mixture and deposited onto the MALDI plate and then analyzed, and no significant differences in the MALDI-TOF MS spectra of these samples were found. In a second series of experiments, matrix (HABA, HAR) and AgTFA were dissolved in THF, and then the solvent was evaporated. The resulting solid mixtures were analyzed by FT-IR. No occurrence of new peaks or shifts compared to those of matrix and AgTFA was found, which indicates no specific interactions between the matrix and AgTFA in the solid phase. Taking these results into account, these observations also support the conclusion of Rashidzadeh et al.,¹⁴ that is, that the gas-phase formation of silver-cluster ions seems

to be the most probable. The source of silver clusters in MALDI is originally present as Ag^+ (in AgTFA), different from the case of those experiments in which neutral metals are employed, for example, in laser ablation or ion-bombardment studies. Therefore, it is obvious that reduction of Ag^+ to Ag in the gas-phase should take place to form cluster ions under MALDI conditions. Now we consider the thermodynamic possibilities of the reduction of Ag^+ in the plume. One of these potential ways is the reaction of silver ions with the neutral matrix molecules (M) as follows:

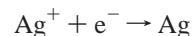


The free energy (ΔG) of the above reaction is given as $\Delta G = \text{IP}(\text{M}) - \text{IP}(\text{Ag})$, where $\text{IP}(\text{M})$ and $\text{IP}(\text{Ag})$ are the ionization potentials of the matrix and the silver, respectively. The IP's of the most commonly used polar organic matrixes were found in the range 8–9 eV,²⁹ and this value for silver is 7.6 eV;³⁰ that is, reaction r1 is endothermic with $\Delta G \cong 0.4$ –1.4 eV. However, reaction r1 may take place considering the collisions with energy 1.5 eV or more^{31,32} in the early phase of plume expansion. Another possibility for the charge-transfer involves the reaction of excited matrix molecules (M^*) with silver ions:



With absorption of a quantum of 337 nm (3.68 eV) by matrix molecules, and considering the high-frequency collisions in the dense plume, the excited matrix molecules are also able to reduce the charge state of silver ions.

The third possible reaction is based on the photoionization of the matrix by absorption of two quanta (2×3.68 eV), as depicted below:



The photoionization of the matrix results in the formation of free electrons that are captured by the silver ions. However, the possibility of reaction r3 may be rather low, due to the low efficiency of photoionization and the capture of electrons by the matrix molecules.

If reaction r2 is in operation under MALDI conditions, it is expected that the number of excited matrix molecules would increase with the increasing laser fluence. Indeed, at low laser fluence no significant cluster ion formations were observed. Figure 8 shows the MALDI-TOF MS spectra of the mixtures of HABA/AgTFA and DIT/AgTFA acquired at low laser fluence.

As seen in Figure 8, besides the protonated and the sodiated matrix peaks ($[\text{M} + \text{H}]^+$, $[\text{M} + \text{Na}]^+$) and some fragment peaks, the formation of $[\text{M} + \text{Ag}]^+$ adduct ions can be observed. On the other hand, in the case of HABA (a) very weak signals originated from the free or “naked” $^{107}\text{Ag}^+$ and $^{109}\text{Ag}^+$ isotopes can be found in the MALDI-TOF MS spectrum as compared to those of DIT (b). As a general observation, formation of $[\text{M} + \text{Ag}]^+$ adduct ions was recognized in the case of all of the 10 matrixes investigated. The absence or very weak signal of “naked” silver ions was observed at low laser fluence in the case of HABA, HAR, and IAA, that is, with those matrixes which produce the strongest cluster ion signals at high laser fluence. These observations indicate that the silver ions are almost completely captured by HABA, HAR, and IAA, reflecting strong interaction of silver ions with these matrixes. We also concluded from these results that the gas-phase reduction

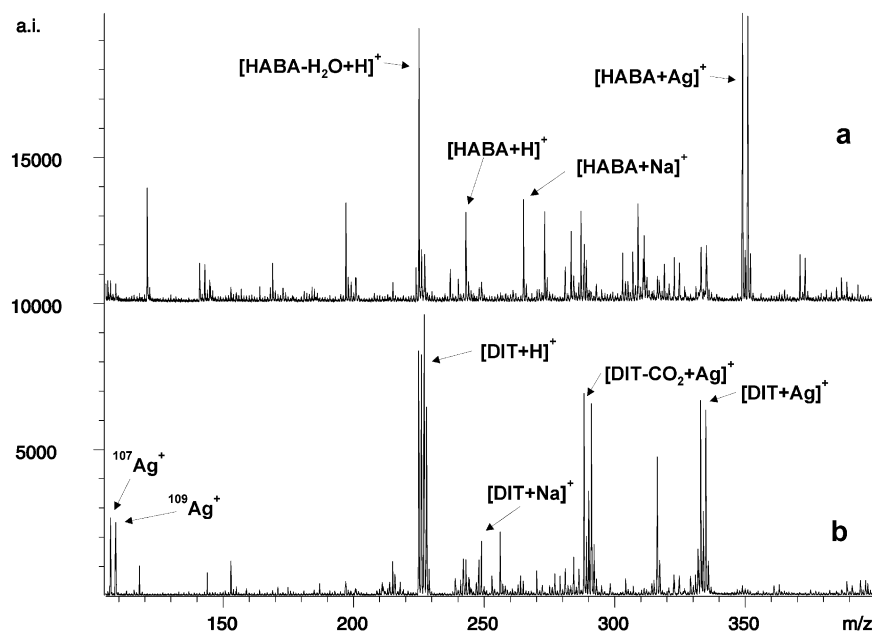


Figure 8. MALDI-TOF MS spectrum of a mixture of HABA and AgTFA (a), and DIT and AgTFA (b) recorded in the positive reflectron mode at low laser fluence. Experimental conditions: see Table 1 caption

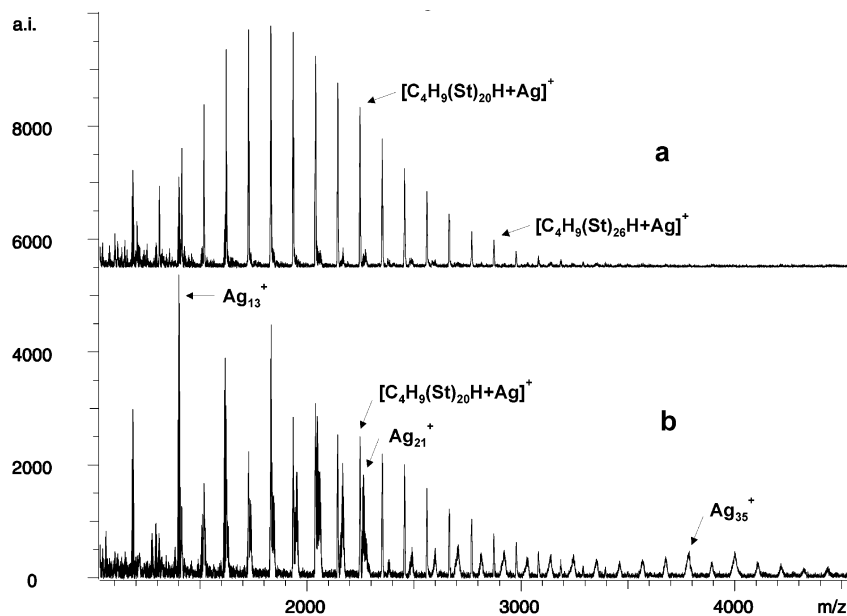


Figure 9. LDI-TOF MS spectra of a mixture of PS and AgTFA (a), and PS, AgTFA, and HABA (b). Experimental conditions: (a) 5:1 (v/v) mixture of PS (0.01 M) and AgTFA (0.09 M) solutions, respectively; (b) 10:2:1 (v/v) mixture of PS (0.01 M) and AgTFA (0.09 M) and HABA (0.08 M) solutions, respectively.

of silver ions may proceed via $[M + Ag]^+$ adduct ions. The HAR is also an effective matrix for production of silver clusters. As it turned out from the low mass MALDI-TOF MS spectrum of the mixture of HAR and AgTFA, significant formation of adduct ions was found, which also indicates that the silver ions interact strongly, most probably with the nitrogen atoms of HAR. The formation of negatively charged silver cluster ions may be explained in a manner similar to that for reaction r2; that is, the silver atom or the neutral silver clusters gain electrons from the excited matrix molecules. It is reasonable, however, to expect higher signal intensity for the positive cluster ions than for the negative ones, owing to the high concentration of Ag^+ and $[M + Ag]^+$ ions. As expected, higher signal intensities were found for positively charged cluster ions than for the negative ones in each case. In the next experiment, the interference between the formation of silver cluster ions and

those of the polystyrene (PS) + Ag^+ adduct ions was investigated. Figure 9 shows the LDI-TOF MS spectra of PS/AgTFA (a) and PS/AgTFA/HABA (b) mixtures.

As seen in Figure 9a, in the absence of matrix, peaks of PS cationized with silver ions appeared, and besides these ions, no significant formation of larger silver cluster ions can be observed. By adding HABA to the mixture of PS/AgTFA in much lower molar ratio than is usual in MALDI, silver cluster ions appeared (Figure 9b). We interpret this result as the enhanced reduction of silver ions by the matrix. The spectra presented in Figure 9 were recorded under the same experimental conditions. The same number of spectra from different spots were acquired to minimize the differences in the ion intensity originated from sample inhomogeneity. Taking these into account, it can be safely stated that PS signals decreased upon addition of the matrix (approximately by one-third). This

observation can be explained as follows: the concentration of Ag^+ available for the cationization of PS is decreased by their reduction with the matrix, which results in the decrease of the concentration of $[\text{PS} + \text{Ag}]^+$ adduct ions, that is, in the decrease of the signal intensity of PS peaks. It should be kept in mind, however, that the amount of added matrix is very small, so it could not effectively assist the desorption of PS. This observation is in good agreement with those of others, namely, Ag^+ salts are the least effective cationization agents for nonpolar polymers when DHB or HABA is used as the matrix.¹⁵ All of the results presented in this article allowed us to conclude that the primary role of the matrix is its capability to reduce the Ag^+ ions to Ag under MALDI conditions. The secondary role, which has not been emphasized yet, is that the matrix may act as a "carrier gas" in the first stage of the plume expansion; that is, it facilitates the growth of clusters.

Conclusions

We investigated the silver cluster ion formation from AgTFA in the presence of different polar organic matrixes under MALDI conditions. The odd–even oscillations in the ion intensity and the magic numbers predicted by the jellium model theory were observed irrespectively of the matrix used. It was also recognized, however, that the matrix greatly influences the cluster ion abundances. Strong cluster ion signals were produced with HABA, HAR, and IAA, but among these matrixes, HABA yields the most abundant cluster ions with the highest resolved cluster number of $n \cong 200$. The highest observable magic numbers in this work are 139 and 137 for Ag_n^+ and Ag_n^- cluster ions, respectively. The mixture of HABA and AgTFA proved to be an effective source of cluster ions in MALDI, which can be utilized by mass selection of specific size for the study of cluster ion–molecule reactions and/or fabricating nanodevices. On the other hand, however, when the analysis of nonpolar polymers with silver ion cationization is the focus, application of HABA, HAR, or IAA is disadvantageous due to the extensive cluster ion formation by these matrixes. On the basis of the experimental results, it can be concluded that excited matrix molecules reduce the silver ions, most probably via adduct ions. It is also reasonable to assume that the matrix can act as a "carrier gas", enhancing the growth of the clusters. The fragmentation behaviors of different cluster ions under MALDI conditions are in line with those experienced by other methods.

Acknowledgment. This work was financially supported by grants Nos. T 037448, T 042740, M 28369 and M 36872 given by OTKA (National Foundation for Scientific Research Development, Hungary), and by the Békésy György Fellowship. The authors also would like to express their thanks to CELLADAM Ltd., Hungary for providing the BIFLEX III MALDI-TOF MS instrument.

References and Notes

- (1) Fournier, R. *J. Chem. Phys.* **2001**, *115*, 2165.
- (2) Schaffner, M. H.; Patthey, F.; Schneider, W. D. *Eur. Phys. J.* **1999**, *D9*, 609.
- (3) Hagen, O. F. Z. *Phys.* **1991**, *D20*, 425.
- (4) Rabin, I.; Jackschath, C.; Sculze, W. Z. *Phys.* **1991**, *D19*, 153.
- (5) Dots, T.; Duncan, M. A.; Powers, D.; Smalley, R. E. *J. Chem. Phys.* **1981**, *74*, 6511.
- (6) Bondebey, V. E.; English, J. H. *J. Chem. Phys.* **1982**, *76*, 2165.
- (7) Weidele, H.; Vogel, M.; Herlert, A.; Krückeberg, S.; Lievens, P.; Silverans, R. E.; Walther, C.; Schweikhard, L. *Eur. Phys. J.* **1999**, *D9*, 173.
- (8) Katakuse, I.; Ichihara, T.; Fujita, Y.; Matsuo, T.; Sakurai, T.; Matsuda, H. *Int. J. Mass Spectrom. Ion Processes* **1986**, *74*, 33.
- (9) Katakuse, I.; Ichihara, T.; Fujita, Y.; Matsuo, T.; Sakurai, T.; Matsuda, H. *Int. J. Mass Spectrom. Ion Processes* **1985**, *67*, 229.
- (10) Krückeberg, S.; Dietrich, G.; Lützenkirchen, K.; Schweikhard, L.; Walther, C.; Ziegler, J. *Eur. Phys. J.* **1999**, *D9*, 169.
- (11) Staudt, C.; Heinrich, R.; Wucher, A. *Nucl. Instrum. Methods Phys. Res., Sect. B: Beam Inter. Mater. Atoms* **2000**, *164*, 677.
- (12) Karas, M.; Hillenkamp, F. *Anal. Chem.* **1988**, *60*, 2299.
- (13) Tanaka, K.; Waki, H.; Ido, Y.; Akita, S.; Yoshida, T. *Rapid Commun. Mass Spectrom.* **1988**, *2*, 151.
- (14) Rashidzadeh, H.; Guo, B. *Chem. Phys. Lett.* **1999**, *310*, 466.
- (15) Macha, S. F.; Limbach, P. A.; Hanton, S. D.; Owens, K. G. *J. Am. Soc. Mass Spectrom.* **2001**, *12*, 732.
- (16) Belu, A. M.; DeSimone, J. M.; Linton, R. W.; Lange, G. W.; Friedman, R. M. *J. Am. Soc. Mass Spectrom.* **1996**, *7*, 11.
- (17) Yalcin, T.; Schriemer, D. C.; Li, L. *J. Am. Soc. Mass Spectrom.* **1997**, *8*, 1220.
- (18) Kéki, S.; Deák, Gy.; Mayer-Posner, F. J.; Zsuga, M. *Macromol. Rapid Commun.* **2000**, *21*, 770.
- (19) Spengler, B.; Kirsch, D.; Kaufmann, R. *Rapid Commun. Mass Spectrom.* **1991**, *5*, 198.
- (20) Spengler, B.; Kirsch, D.; Kaufmann, R.; Jaeger, E. *Rapid Commun. Mass Spectrom.* **1992**, *6*, 105.
- (21) Mamyurin, B. A.; Karataev, V. I.; Shmikk, D. V.; Zagulin, V. A. *Sov. Phys. JETP* **1973**, *37*, 45.
- (22) Deák, Gy.; Zsuga, M.; Kelen, T. *Polym. Bull.* **1992**, *29*, 239.
- (23) Knight, W. D.; Clemenger, K.; de Heer, A. W.; Sauder, A. W.; Chou, M. Y.; Cohen, M. L. *Phys. Rev. Lett.* **1984**, *52*, 2141.
- (24) Krückeberg, S.; Dietrich, G. M.; Lützenkirchen, K.; Schweikhard, L.; Walther, C.; Ziegler, J. *Int. J. Mass Spectrom. Ion Processes* **1996**, *155*, 141.
- (25) Krückeberg, S.; Dietrich, G. M.; Lützenkirchen, K.; Schweikhard, L.; Walther, C.; Ziegler, J. *J. Chem. Phys.* **1999**, *110*, 7216.
- (26) Hild, U.; Dietrich, G.; Krückeberg, S.; Lindinger, M.; Lützenkirchen, K.; Schweikhard, L.; Walther, C.; Ziegler, J. *Phys. Rev. A* **1998**, *57*, 2786.
- (27) Dzhe-milev, N. K.; Rasulev, U. K.; Verkhoturov, S. V. *Nucl. Instrum. Methods* **1987**, *B29*, 531.
- (28) Morse, M. D. *Chem. Rev.* **1986**, *86*, 1049.
- (29) Karbach, V.; Knochenmuss, R. *Rapid. Commun. Mass. Spectrom.* **1998**, *12*, 968.
- (30) Look, H.-P.; Beaty, L. M.; Simard, B. *Phys. Rev. A* **1999**, *59*, 873.
- (31) Zenobi, R.; Knochenmuss, R. *Mass Spectrom. Rev.* **1998**, *17*, 337.
- (32) Knochenmuss, R.; Stortelder, A.; Breuker, K.; Zenobi, R. *J. Mass Spectrom.* **2000**, *35*, 1237.